Power-Law-Like Stress Relaxation of Block Copolymers: Disentanglement Regimes

Michael Rubinstein*

Corporate Research Laboratories, Eastman Kodak Company, Rochester, New York 14650-2110

S. P. Obukhov

Landau Institute for Theoretical Physics, Moscow, Russia, and Department of Physics, University of Florida, Gainesville, Florida 32611

Received September 11, 1992; Revised Manuscript Received December 17, 1992

ABSTRACT: We consider stress relaxation in a strongly segregated lamellar mesophase, where block copolymers are in the "brush" state with junction points confined to the interface between the adjacent lamellae and blocks stretched out away from it. If the molecular weight of the blocks is large enough, they entangle with their neighbors as well as with blocks from the opposite brush. The number of entanglements of one particular chain with the opposite brush varies from chain to chain even in the monodisperse system. We demonstrate that this dispersion of the number of entanglements leads to a very broad spectrum of relaxation times and to an effectively power-law-like stress relaxation function $\log G \sim (\log t)^{\alpha}$ with $\alpha = 1/2$ ($\alpha = 2$) in the strong (weak) chain-stretching limit. We analyze various disentanglement mechanisms for diblocks and triblocks and the onset of the diffusion of copolymers along the interface. Another relaxation mechanism is due to the displacement of a block across the interface into the "enemy" phase. We conclude that for highly entangled copolymers it will be an important mode of stress relaxation (especially for triblock copolymers). For asymptotically long times the relaxation of stress along the perfectly ordered lamella will be liquidlike. In a system with defects in domain structure the relaxation of stress is controlled by the processes of equilibration of excess density along the layers. For the lamellar mesophase we found $G(t) \sim t^{-1/2}$, while for the cylindrical mesophase, $G(t) \sim t^{-1/4}$.

I. Introduction

Block copolymers, i.e., macromolecules composed of sequences of chemically distinct monomers, have a remarkably rich spectrum of properties and applications.[1] The sequences or monomers, called blocks, are often incompatible, but, being covalently bonded together in a block copolymer, they cannot macrophase-separate and instead form domain structures called mesophases.[2] The morphology of these mesophases depends on the relative size of the blocks and the architecture of the molecules.[2] For example, strongly asymmetric diblocks form spherical micelles, while symmetric blocks lead to a lamellar mesophase.

These structures dramatically affect the rheological response of the system, especially at long times. Recently, it was suggested[3] that rheology is the best way to distinguish between ordered (microphase-separated) and disordered (microscopically mixed) states of block copolymers.

The viscoelastic response in the microscopically mixed state is that of a polymer liquid with a well-defined terminal relaxation time,[3,4] but the response in the microphase-separated state is truly remarkable.[3,4] The storage modulus G' and the loss modulus G'' have a power-law-like frequency dependence

$$G'(\omega) \sim G''(\omega) \sim \omega^{\alpha} \qquad (1)$$

where α slowly changes between 0.3 and 0.7 in the frequency range of over 10 decades.[5] This response is intermediate between that of a liquid (with low-frequency limiting behavior $G' \sim \omega^2$ and $G'' \sim \omega^1$) and that of a solid [*with nonzero* low-frequency limiting storage modulus $G'(\omega) \to \text{const} \neq 0$ as $\omega \to 0$].

There are two possible mechanisms of this anomalous behavior: microscopic and mesoscopic. We believe that both are responsible for the power-law-like behavior in high molecular weight block copolymers, but in different frequency intervals. The microscopic mechanism of this unusual relaxation behavior is due to the nontrivial disentanglement processes and is the subject of the present paper. The mesoscopic mechanism is due to the deformation and displacement of domains (lamellae, cylinders, etc.) and will be briefly commented upon in section V and addressed in detail in a future publication.[6] We expect this mechanism of redistribution of defects in the domain structure to be responsible for the power-law behavior at the lowest frequencies. In a lower molecular weight (unentangled) system this mesoscopic mechanism is the only source of the unusual viscoelastic response (eq 1).

The importance of entanglements for stress relaxation in lamellar structures was pointed out by Witten, Leibler, and Pincus.[7] These authors made an estimate of the characteristic relaxation times due to the disentanglement process in these systems. We demonstrate below that the relaxation modes described in ref 7 are only the high-frequency part of a broad relaxation spectrum. The main reason is that the number of entanglements fluctuates from chain to chain. These fluctuations combined with the exponential dependence of the relaxation time on this number of entanglements lead to the power-law-like relaxation.

In section II we briefly review the configurational properties of polymers in a lamellar mesophase and the extent of the interpenetration of blocks from the neighboring lamellae.[7] In section III we consider the effect of fluctuations of the number of entanglements on the stress relaxation in the interpenetration zone. In section IV we discuss the transformation of the viscoelastic response of a lamella from solidlike at shorter times to liquidlike at longer times. In section V we analyze the reequilibration of copolymer density per unit area of interface in systems with defects in domain structure and demonstrate that it leads to a power-law stress relaxation behavior. In section

0024-9297/93/2226-1740$04.00/0

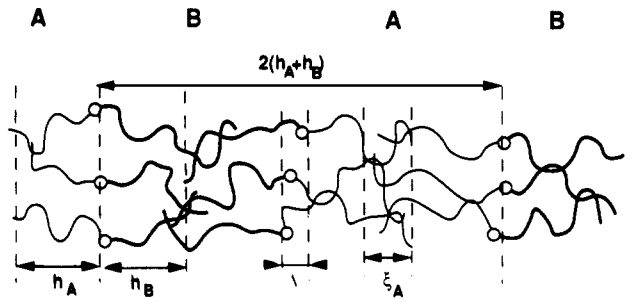

Figure 1. Block copolymers in a lamellar mesophase. The thicknesses of A and B lamellae are $2h_A$ and $2h_B$, respectively. The width of the interface between A and B regions is Δ. The widths of the A and B interpenetration zones are ξ_A and ξ_B, respectively.

VI we summarize the results of the paper and compare them with recent experiments.

II. Statics of the Dry Brush State

In this section we review the main results[7-14] of the equilibrium static configurations of block copolymers in the lamellar mesophase that are used in our dynamic theory.

The domains are formed as a result of the repulsive interactions between the A and B blocks of the copolymer. In the strongly segregated case, the contacts between the unlike blocks are limited to the narrow interface region. This interface is similar to the one between A-rich and B-rich domains in an immiscible blend of homopolymers A and B. The energy cost of an A subsection penetrating a B-rich domain should be comparable to the entropy gain ($\sim kT$). The B subsection penetrating an A-rich domain has similar energy loss and entropy gain. The interface contains a mixture of such A and B subsections. The number of monomers in a typical subsection is g, with the energy proportional to $kT\chi g \approx kT$ and thus $g \approx 1/\chi$, where χ is the Flory interaction parameter. The width of the interface is $\Delta \approx bg^{1/2} \approx b\chi^{-1/2}$, where b is an effective bond length. A more precise estimate[12] leads to

$$\Delta = 2b(6\chi)^{-1/2}$$

Block copolymers have their junction points near the interface and, without solvent, form "dry brushes", as sketched in Figure 1 (see section III.D for the discussion of fluctuations of junction points away from the interface). The energetically favorable decrease of the interface area leads to entropically unfavorable chain stretching due to the excluded-volume effects (density constraints). The equilibrium lamellar thickness $2(h_A + h_B)$, where h_A and h_B are the heights of A and B brushes (Figure 1), is determined by the balance between the two energies:

(i) The interface energy per molecule is $\sigma\gamma$, where σ is the interface area per molecule

$$\sigma = (N_A + N_B)/[(h_A + h_B)\rho_0] \qquad (2)$$

with the degree of polymerization of A and B blocks denoted by N_A and N_B, the number of monomers per unit volume denoted by ρ_0, and the surface tension $\gamma \approx kT\chi\Delta\rho_0 \approx kT\chi^{1/2}b\rho_0$. A more complete theory[12] gives the surface tension

$$\gamma = kT(\chi/6)^{1/2}b\rho_0 \qquad (2a)$$

(ii) The stretching energy of a Gaussian coil of unperturbed size $R_i \approx bN_i^{1/2}$ where i is an index of a block (i = A or B), elongated to size h_i is $3kTh_i^2/(2R_i^2)$.

Minimization of the free energy per molecule (neglecting the logarithmic term due to localization of junction points)

$$F/kT = (\chi/6)^{1/2}(N_A + N_B)b/(h_A + h_B) + 3h_A^2/(2N_Ab^2) + 3h_B^2/(2N_Bb^2) \qquad (3)$$

with respect to the heights of both brushes h_A and h_B leads to an estimate of these heights

$$h_i = bf_i(\chi/54)^{1/6}N^{2/3} \qquad \text{where } i = \text{A or B} \qquad (4)$$

and $f_i = N_i/N$ is the fraction of the monomers of type i ($f_A + f_B = 1$). The period of the lamellar structure for a copolymer with the total degree of polymerization $N = N_A + N_B$ is

$$2(h_A + h_B) = b(32\chi/27)^{1/6}N^{2/3} \approx 1.03bN^{1/2}(\chi N)^{1/6} \qquad (4a)$$

Note that in order to achieve any significant chain stretching one needs very large values of the parameter χN ($\chi N \gg 100$).

The actual stretching of the copolymer is not uniform—the sections near the junction point are extended more than the ones near chain ends.[13,14] The nonuniform tension in a system with constant monomer density can only be achieved if there is a distribution of chain ends throughout the lamellar thickness. A more accurate treatment,[13] that self-consistently takes into account this distribution, leads to a prefactor $\pi^2/8$ instead of $3/2$ in the stretching part of the free energy (eq 3) and results in a slight modification of prefactors in eqs 4 and 4a:

$$h_i = bf_i(8\chi/3\pi^4)^{1/6}N^{2/3} \qquad \text{where } i = \text{A or B} \qquad (4b)$$

$$2(h_A + h_B) \approx 1.10bN^{1/2}(\chi N)^{1/6} \qquad (4c)$$

For example, the period of a lamellar mesophase of a symmetric copolymer with $\chi N = 400$ is $2(h_A + h_B) \approx 3.0bN^{1/2}$.

The self-consistent conformational model[13,14] predicts the free energy of an A monomer in an A domain (or B monomer in a B domain) a distance z from the interface of the lamella in the strong stretching limit to be

$$\mu_i(z) = (3\pi^2/8)kT(h_i^2 - z^2)/(N_i^2b^2) \qquad \text{with } i = \text{A or B} \qquad (5)$$

This free energy can be understood as the cost of bringing an A monomer (or a B monomer) from the middle of the lamella $z = h_A$ ($z = h_B$) to the distance z from the interface and is quite large everywhere except near the middle of the lamella $z \approx h_A$ ($z \approx h_B$).

The dynamic coupling between the neighboring lamellae depends on the degree of interpenetration of the blocks. The method of estimation of the width of the interpenetration zone is similar to that for the width of the interface between A and B lamellae.[7] One needs to determine the length q_i of a chain subsection (say from the opposite brush) with the energy $\sim kT$ in this potential.[7] This subsection of a chain in such a weak potential stays with its nearly unperturbed Gaussian size $bq_i^{1/2}$. The monomeric free energy $\mu_i(z)$ (eq 5) in this Gaussian interpenetration region ($h_i - z \ll h_i$) can be approximated as

$$\mu_i(z) \approx (3\pi^2/4)kTh_i(h_i - z)/(b^2N_i^2) \qquad \text{where } i = \text{A or B} \qquad (6)$$

The energy per typical monomer of the inserted chain (with $h_i - z \approx bq_i^{1/2}$) is

$$(3\pi^2/4)kTh_iq_i^{1/2}/(bN_i^2) \approx 2^{-3/2}3^{5/6}\pi^{4/3}kT\chi^{1/6}q_i^{1/2}/(N_iN^{1/3}) \qquad \text{where } i = \text{A or B} \qquad (7)$$

and we have used eq 4b for the height of a brush. The

number of monomers q_i on a typical overlapping section of a chain is determined by the condition

$$2^{-3/2}3^{5/6}\pi^{4/3}kT\chi^{1/6}q_i^{3/2}/(N_iN^{1/3}) \approx kT \qquad \text{where } i = \text{A or B} \quad (8)$$

leading to

$$q_i = c_1\chi^{-1/9}N_i^{2/3}N^{2/9} \qquad \text{where } i = \text{A or B} \quad (9)$$

and where we have combined all numerical prefactors into a dimensionless constant

$$c_1 = 2\pi^{-8/9}3^{-5/9} \approx 0.4$$

We can rewrite eq 9 as

$$q_i = c_1N_i(\chi N)^{-1/9}f_i^{-1/3} \qquad \text{where } i = \text{A or B} \quad (9a)$$

Thus the size of the interpenetration zone is[7]

$$\xi_i = 2bq_i^{1/2} = 2c_1^{1/2}bN_i^{1/2}(\chi N)^{-1/18}f_i^{-1/6} \qquad \text{where } i = \text{A or B} \quad (10)$$

In the strong stretching limit the interpenetration zone occupies a fraction of a lamella

$$\xi_i/(2h_i) = 3^{-1/9}\pi^{2/9}(\chi N)^{-2/9}f_i^{-2/3} \qquad \text{where } i = \text{A or B} \quad (10a)$$

decreasing with increasing parameter χN. For example, in a symmetric copolymer ($f_i = {}^1/_2$) with $\chi N = 400$ the interpenetration zone occupies approximately half of a lamella.

As mentioned above, the chain ends are distributed throughout the brush. The probability of finding an end in the interval from z to $z + dz$ from the interface is[13]

$$\epsilon_i(z)\,dz = z\,dz/[h_i(h_i^2 - z^2)^{1/2}] \quad (11)$$

The fraction of ends in the interpenetration zone slowly decreases with increasing χN

$$e_i = \int_{h_i - \xi_i/2}^{h_i} \epsilon_i(z)\,dz = [1 - (1 - \xi_i/2h_i)^2]^{1/2} \sim 2^{1/2}3^{-1/18}\pi^{1/9}(\chi N)^{-1/9}f_i^{-1/3} \quad (12)$$

where we have used eq 10a. In the example, considered above ($f_i = {}^1/_2$ and $\chi N = 400$) approximately three quarters of the ends are in the interpenetration zone.

We conclude that in most practical situations block copolymers in the strong segregation (narrow interface) regime are rather weakly stretched $(h_A + h_B)/(bN^{1/2}) \approx 0.55(\chi N)^{1/6}$. Blocks from opposite interfaces heavily overlap with each other (large interpenetration zone) $\xi_i/(2h_i) \approx 1.1(\chi Nf_i^3)^{-2/9}$. Nevertheless, for completeness, we consider below both limits: (1) strong stretching $(h_A + h_B)/(bN^{1/2}) \gg 1$ with narrow interpenetration zone $\xi_i/(2h_i) \ll 1$; and (2) weak stretching $(h_A + h_B)/(bN^{1/2}) = O(1)$ with wide interpenetration zone $\xi_i/(2h_i) = O(1)$.

III. Brush-on-Brush Disentanglement Regime

A. The Model. A Pair of Interpenetrating Dry Brushes. Independent of the degree of the copolymer stretching, the sections of blocks in the interpenetration zones are only weakly deformed and their conformation is almost Gaussian, analogous to that of a homopolymer in the melt. These sections are entangled,[15] as long as they are of high enough molecular weight ($q_i > N_{ie}$, with N_{ie} being the average number of monomers in an entanglement strand of a block of type i). Note that we use the homopolymer values for N_{ie} that should be applicable in the interpenetration zone but could be different for each of the two components (N_{Ae} need not be equal to N_{Be}).

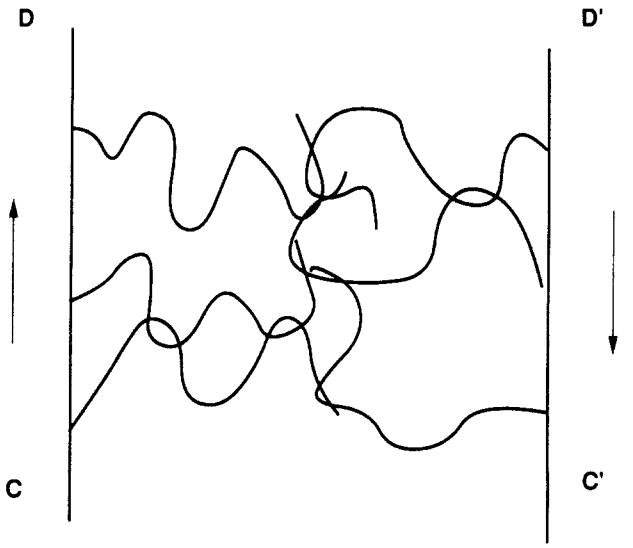

Figure 2. Brush-on-brush model. The junction points are fixed at the interfaces CD and C′D′. Arrows indicate the direction for a simple shear.

Each component could have a different average number of entanglements in the interpenetration zone (q_A/N_{Ae} and q_B/N_{Be}) and different monomeric friction coefficients (different Rouse times of entanglement strands t_{Ae} and t_{Be}). Therefore, the disentanglement rates for the pairs of brushes in the two interpenetration zones (A and B) could be quite different. The faster of the two rates determines the zone (for definiteness, let it be zone A) where the lamellae first begin to slip by each other. This process will be described in detail in the present section, while the relaxation of the remaining entanglements and the onset of the two-dimensional flow within each domain will be addressed in section IV.

We assume that the initial disentanglement processes in each half of a lamella (an A zone and a B zone) are independent from each other and the junction points of the blocks are localized near the interface. Each half of the lamella (an A region and a B region) can be modeled by a pair of interpenetrating dry brushes (Figure 2). We will discuss the validity of this decoupling approximation and the importance of the fluctuations of a junction point away from the interface in section III.D.

Let us consider stress relaxation after a step-strain applied at time $t = 0$ along the lamellar plane (Figure 2). The two brushes CD and C′D′ are shifted with respect to each other due to the imposed strain. Stress relaxation can only occur as the molecules from the opposite brushes begin to disentangle by the fluctuations of the length of their confining tubes.[7] These relaxation modes are analogous to the arm retraction modes in the melt or concentrated solution of star polymers.[15-19]

The longest relaxation time of a star polymer τ_{star} depends exponentially on the number of entanglements N_a/N_e per arm[15-19]

$$\tau_{star} \approx t_e \exp(\nu N_a/N_e) \quad (13)$$

where N_a is the degree of polymerization of an arm, ν is a constant of order unity ($\nu \approx 0.6$), and t_e is the Rouse time of an entanglement strand (of N_e monomers).[18] The reason for this extremely slow relaxation is the entropically unfavorable configurations arms of a star have to get into in order to disentangle. The further the entanglement is from the tip of an arm, the harder it is for the star polymer to remove it. The time it takes to release the entanglement

number s (numbers start at the arm's tip) is[15,17-19]

$$t(s) = t_e \exp(\nu s^2 N_e/N_a) \quad (14)$$

The same behavior is expected for the disentanglement of blocks with junction points localized near the interface[7] (for the pair of brushes sketched in Figure 2). If all A chains have the same number of entanglements in the overlap region $n_A = q_A/N_{Ae}$ (where the number q_A of monomers in the interpenetration zone is given by eq 9a)

$$n_A = c_1(N_A/N_{Ae})(\chi N_A)^{-1/9} f_A^{-2/9} \quad (15)$$

then the characteristic relaxation time after a step strain along the lamellae would be[7]

$$t_A^* = t(n_A) = t_{Ae} \exp[\nu c_1^2 f_A^{-4/9}(N_A/N_{Ae})(\chi N_A)^{-2/9}] \quad (16)$$

We are concentrating on the interpenetration zone A in this section because we assume that the disentanglement process in that region is faster than that in the zone B ($t_A^* < t_B^*$). The relaxation time t_A^* determines the long-time behavior ($t > t_A^*$) of the stress relaxation function $G(t)$ for shear along the lamellar plane in the analysis of ref 7

$$G(t) \sim \exp(-t/t_A^*) \qquad \text{for } t > t_A^* \quad (17)$$

What is important in our consideration is that the number of entanglements m in the interpenetration zone is not the same for all chains: there is always some dispersion in m due to thermal fluctuations. Another source of dispersion in m is the polydispersity of polymers to be discussed in section VI. We shall see below that the dispersion in the number of entanglements, together with the exponentially strong dependence of relaxation time $t(s)$ on the entanglement number s (eq 14), leads to a completely different time dependence of the stress relaxation function $G(t)$ than that of eq 17. This is analogous to the effect of the distribution of entangled dangling ends on the stress relaxation function of polymer networks.[20]

B. Fluctuations in the Number of Entanglements in the Interpenetration Zone. We study the dispersion due to thermal fluctuations in a monodisperse system by considering the two limiting cases: strong and weak stretching of chains.

1. Strong Stretching Limit. The strong stretching case can be achieved for very high molecular weight polymers and strong repulsion between blocks ($\chi N \gg 100$). In this case, the interpenetration zone occupies only a small fraction of a lamella (eq 10a). The fraction of A blocks that reach this region, e_A, is also small for very large χN (eq 12). The number of monomers of each A block present in the interpenetration zone differs from chain to chain with the average given by eq 9a. This dispersion and the resulting distribution in the number m of entanglements in the interpenetration zone for A blocks that reach it can be described by the exponential distribution

$$P_s(m) \approx [\exp(1/n_A) - 1] \exp(-m/n_A) \quad (18)$$

where the average number of entanglements in this zone is $1/[1 - \exp(-1/n_A)] \approx n_A$ for large n_A (see eq 15 for the value of n_A). Note that this average is taken over a small fraction e_A of A blocks that actually reach this zone, but not over all A blocks.

The fluctuations in the number of monomers between entanglements are not important in this case because they lead to a Poisson distribution (see section III.B.2) that for long chains is much narrower than the exponential one (eq 18).

2. Weak Stretching Limit. In the case of weak stretching with a heavy overlap of the opposite brushes, the size of the interpenetration zone is close to the spacing between inerfaces ($\xi_A \approx 2h_A$). The average number of entanglements per chain in this overlapping zone is roughly equal to the total number of entanglements per A block N_A/N_{Ae}, but the actual number of entanglements m in an A block fluctuates around this average number even in the monodisperse case. The reason is that different chains have different configurations and the number of monomers between entanglements is a random variable. In this case, the fluctuations in the number of entanglements per chain are characterized by a Poisson distribution

$$P_w(m) = \exp(-N_A/N_{Ae})(N_A/N_{Ae})^m/m! \quad (19)$$

where $P_w(m)$ is the probability of an A block to have m entanglements (they are all in the interpenetration zone). This distribution is a result of the fluctuation of the number of monomers between entanglements. Note that this dispersion of the number of entanglements per chain exists in ordinary polymer melts and solutions. It is called tube length fluctuation[15] and is responsible for the anomalous 3.4 power-law dependence of the viscosity of linear entangled polymers on their molecular weight.[21,22] The consequences of this fluctuation in the number of entanglements per chain are much more dramatic in some block copolymer systems due to the spatial constraints caused by the domain geometry, as will be demonstrated below.

C. Disentanglement Process in the Interpenetration Zone. If we know the distribution in the number of entanglements per chain in both the strong (eq 18) and the weak (eq 19) stretching limits, we can construct the stress relaxation function of block copolymers for a simple shear along the lamellar planes (Figure 2). Recall the stress relaxation function for stars with N_a monomers per arm[18]

$$G(t) = G_0[1 - s(t)N_e/N_a]^2 \qquad \text{for } t < \tau_{star} \quad (20)$$

where $s(t)$ is the number of relaxed entanglements per arm at time t. The second power of the bracket is the result of the self-consistent approximation[18,23] of the constraint-release (tube renewal) effect on the stress relaxation due to the motion of the chains forming the tube. By analogy with star polymers (eq 20), the remaining stress for the pair of brushes (Figure 2) is proportional to the square of the fraction of unrelaxed entanglements in the interpenetration zone.

1. Strong Stretching Limit. In the strong stretching case we neglect fluctuations in the number of entanglements per block and only consider the dispersion in the fraction of them in the interpenetration zone $P_s(m)$ (eq 18) for those A blocks that reach this zone. As we stated in the beginning of the section, we concentrate on the A brush because it is assumed that A blocks disentangle faster than B blocks (they can have fewer entanglements or a lower friction coefficient). After a step strain, the number of relaxed entanglements at time t is approximately the same for each block and can be obtained by inverting eq 14

$$s(t) = [N_A/(N_{Ae}\nu)]^{1/2}[\ln(t/t_{Ae})]^{1/2} \quad (21)$$

For a simple shear along the plane of the brushes we are only interested in the disengaged entanglements that are in the interpenetration zone. In the case of strong stretching the stress relaxation function can be obtained

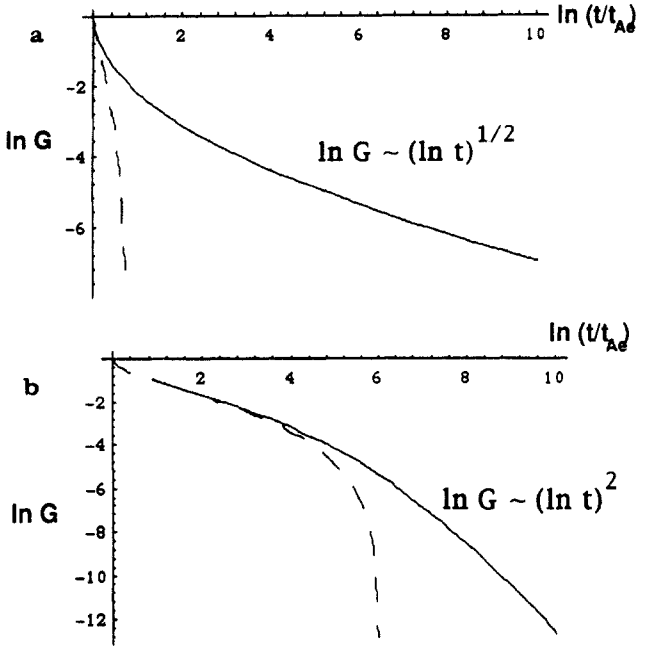

Figure 3. (a) Stress relaxation in the strong stretching limit for symmetric copolymer ($f_A = 1/2$) with $\chi N_A = 200$ and $N_A/N_{Ae} = 20$ entanglements. The solid curve is a plot of the stress relaxation function with fluctuations in the number of entanglements in the interpenetration zone (eqs 23 and 24 with $c_1 \approx 0.4$). The dashed curve is a plot of the stress relaxation function without these fluctuations. (b) Stress relaxation in the weak stretching limit for $N_A/N_{Ae} = 10$ entanglements in an A block. The solid curve is a plot of the stress relaxation function with fluctuations in the number of entanglements in an A block. The dashed curve is a plot of the stress relaxation function without these fluctuations.

by combining eqs 18 and 20

$$G_s(t) = G_0\left\{1 - \left(1 - \exp\left(-\frac{1}{n_A}\right)\right)\left[\sum_{m=1}^{s(t)} mP_s(m) + s(t)\sum_{m=s(t)+1}^{\infty} P_s(m)\right]\right\}^2 \quad (22)$$

Here the coefficient in front of the square bracket is a normalization factor (see eq 18). The average number of entanglements per block in the interpenetration zone n_A is given by eq 15. The first term in the square bracket is the average number of entanglements on the completely relaxed sections of A blocks in the interpenetration zone [those that have $m \le s(t)$ entanglements there]. The second term corresponds to the longer sections in this zone that are only partially relaxed [out of m entanglements in the zone they have only $s(t)$ relaxed ones]. Sums over the exponential distribution are easily evaluated to yield

$$G_s(t) = G_0 \exp[-2s(t)/n_A] = G_0 \exp\{-c[\ln(t/t_{Ae})]^{1/2}\} \quad (23)$$

where

$$c = (2f_A^{2/9}/c_1\sqrt{\nu})(N_A/N_{Ae})^{-1/2}(\chi N_A)^{1/9} \quad (24)$$

As an example, consider a symmetric copolymer ($f_A = 1/2$) with $\chi N_A = 200$ and $N_A/N_{Ae} = 20$ entanglements. Taking the value $c_1 \approx 0.4$ from section II, we find from eq 15 that, out of these 20 entanglements, there are $n_A \approx 5$ in the interpenetration zone. The numerical coefficient, defined in eq 24, is $c \approx 2.2$. The dependence of the stress relaxation modulus on time is displayed in Figure 3a. The solid curve is a plot (on a log–log scale) of eq 23. The dashed curve is the sketch of the stress relaxation function neglecting the fluctuations in the number of entanglements in the interpenetration zone. On the time scales longer than t_A^* it is an exponentially decaying function (eq 17), while our prediction (eq 23) has a power-law-like behavior with the slope slowly changing from ≈ 1.1 at $\ln(t/t_{Ae}) = 1$ to ≈ 0.35 at $\ln(t/t_{Ae}) = 10$. The cutoffs of this very broad relaxation spectrum are discussed in sections III.D and IV.

2. Weak Stretching Limit. Let us now consider the case of weak copolymer stretching with the probability distribution function $P_w(m)$ (eq 19) of having m entanglements per chain. The number of entanglements $k(t)$ in an A block completely relaxed by time t can be found by inverting eq 13

$$k(t) = (1/\nu)\ln(t/t_{Ae}) \quad (25)$$

The blocks with $m < k(t)$ do not contribute to the elastic modulus at time t. For blocks with $m > k(t)$, the number of relaxed entanglements is given by eq 21 (inverted eq 14)

$$s_m(t) = [(m/\nu)\ln(t/t_{Ae})]^{1/2} \quad (26)$$

The stress relaxation function for a simple shear along the brush (Figure 2) is proportional to the square of the fraction of unrelaxed entanglements (this is a self-consistent approximation of constraint release,[18,23] as discussed below eq 20)

$$G_w(t) = G_0\left\{1 - \frac{N_{Ae}}{N_A}\left[\sum_{m=1}^{k(t)} mP_w(m) + \sum_{m=k(t)+1}^{\infty} s_m(t)\,P_w(m)\right]\right\}^2 \quad (27)$$

The first term in the square brackets is the average number of entanglements per completely relaxed chain, and the second one is the average number of relaxed entanglements on a partially relaxed chain. The first sum over the Poisson distribution can be expressed in terms of the incomplete Γ function

$$G_w(t) = G_0\left\{1 - \frac{\Gamma(k(t),N_A/N_{Ae})}{\Gamma(k(t))} - \frac{N_{Ae}}{N_A}\sum_{m=k(t)+1}^{\infty} s_m(t)\,P_w(m)\right\}^2 \quad (28)$$

In Figure 3b we plot this stress relaxation function (eq 28) for $N_A/N_{Ae} = 10$ (solid curve). It is compared with the stress relaxation function with the same parameters, but without fluctuations in the number of entanglements per chain (eq 20) (dashed line). If fluctuations are neglected, there is a longest relaxation time $t_A \approx 400t_{Ae}$. At longer times the relaxation function (without fluctuations) decays exponentially (eq 17). The long-time asymptotic behavior of the stress relaxation function with fluctuations in the number of entanglements per chain described by eq 28 is

$$\ln G_w(t) \sim [\ln(t/t_{Ae})]^2 \quad (29)$$

with no longest relaxation time.

We did not take into account the fact that chains with an anomalously high number of entanglements would have a very short distance between them and therefore very little stored length to form the unentangled loops necessary for disentanglement. This would slow down the release of entanglements and delay the relaxation of these chains even further.

The anomalous power-law-like stress relaxation behavior (eqs 23 and 29) continues as long as the brush-on-brush model is valid (as long as the junction points are localized

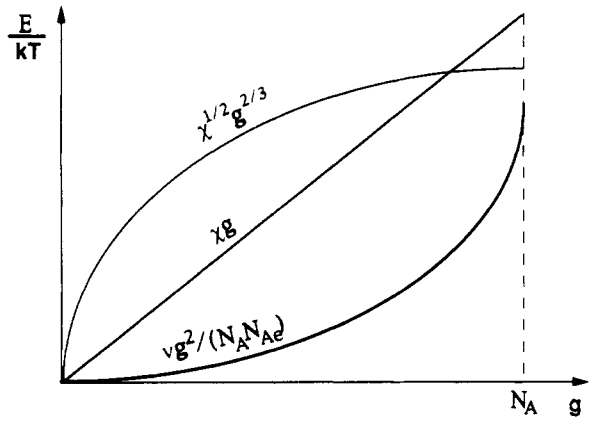

Figure 4. Comparison of arm retraction with fluctuations of an A block into a B zone. The solid curve is an entropic part of a free energy lost in the process of relaxation of the section of an A block with g monomers. The thin lines indicate energy cost for placing g monomers of an A block into a B zone (straight line, without collapse of this section; thin curve, with collapse).

at the interface). The cutoff of this regime can be caused by either transverse or longitudinal displacement of the junction points. The transverse displacement of the junction points is discussed in the next section. The melting of the lamellae and the onset of longitudinal diffusion is described in section IV for both diblocks and triblocks.

D. Fluctuations of an A Block into a B Zone. The brush-on-brush model assumes junction points to be localized at the interface. This assumption is reasonable if the friction coefficient of B lamellae is significantly larger than that of A lamellae (the glass transition of B lamellae is higher and it is effectively "glassy" on the time scales of an A block relaxation).

An additional mode of stress relaxation, which has been neglected so far, is the displacement of a junction point away from the interface. There is an interaction energy cost $kT\chi g$ for moving g monomers of type A into the B zone (assuming that this section does not collapse). Note that this potential is linear in the curvilinear displacement gb (straight thin line in Figure 4), while the entropic potential for the tube length fluctuations is quadratic in the curvilinear length of the retracted subsection $kT\nu g^2/(N_A N_{Ae})$ (thick line in Figure 4). For strongly interacting blocks ($\chi N_{Ae} \gg 1$) the interaction energy cost is much higher than the entropic one (straight thin line is above the thick parabola in Figure 4) and the junction point will be localized near the interface, as was assumed in the model above. For the weaker interacting case ($\chi N_{Ae} \leq 1$) the modes coupling tube length fluctuations with the diving of an A block into a B zone are possible.

If there is strong unfavorable interaction between A and B monomers, larger subsections of an A block in a B layer will be collapsed and the energetic cost will be proportional to the surface of a globule $kT\chi^{1/2}g^{2/3}$ instead of the volume (curved thin line in Figure 4 falls below thin straight line for large g). At early stages of relaxation, partial arm retraction is always a preferred mode (for smaller g thick parabola is below both thin lines in Figure 4). At later stages, the formation of a collapsed A globule in a B region could be energetically more favorable for $g > \chi^{3/2}N_{Ae}^3$ (especially for chains that have more entanglements and smaller N_{Ae}). This relaxation regime with fluctuations of A globules into the B microphase should be important for high enough molecular weights ($N_A \gg \chi^{3/2}N_{Ae}^3$), but there could be other effects slowing down the displacement of a large A globule into a B layer.[24]

The anomalous power-law-like regimes of stress relaxation (eq 23 and 29) are due to fluctuations in the number of entanglements in the interpenetration zone. Blocks with more than an average number of entanglements lead to exponentially longer disentanglement times. But blocks with many entanglements (but the same number of monomers) may "prefer" to relax by displacement into the "enemy" lamella (e.g., A blocks into a B lamella). By equating the entropic and energetic costs of these two different modes of relaxation, we find the largest number of entanglements per block $m_{max} \approx \chi^{1/2}N_A^{2/3}/\nu$ that relax by the "pure arm retraction" mechanism. For blocks with a smaller number of entanglements ($m < m_{max}$) the fluctuations of the junction points away from the interface can be neglected. This largest number of entanglements m_{max} defines the cutoff for the sum in eq 28. For example, blocks with $N_A = 1000$ monomers ($N_A/N_{Ae} = 10$) and Flory interaction parameter $\chi = 0.025$ have an extensive power-law-like regime (over 4 decades of time) due to blocks with a number of entanglements between the average ($m = 10$) and the largest ($m_{max} \approx 26$).

The onset of the transverse diffusion perpendicular to the lamellar planes is controlled by the energy barrier for an A block completely immersing into a B zone[24] $\Delta E_A \sim kT\chi^{1/2}N_A^{2/3}$ (and by the similar barrier for the B block $\Delta E_B \sim kT\chi^{1/2}N_B^{2/3}$). An alternative description for the transverse diffusion has been recently proposed by Helfand.[25] In his picture an A block stretches across a B zone leading to activation energy barrier $\Delta E_A = 4\pi^{-2/3}3^{1/3}kTf_B f_A^{-2/3}(\chi N_A)^{2/3}$. Both mechanisms may be important for different systems at different stages of transverse motion.

In addition to considerations in terms of energy barriers there could be a significantly higher friction coefficient for A sections in a B zone compared to that in an A zone (because B lamellae may have a higher glass transition temperature). This difference in friction coefficients would significantly increase the range of the power-law-like region.

IV. "Melting" of a Lamella

A. Diblock Copolymers. In the previous section we have demonstrated that the stress relaxation function for a simple shear of a pair of interpenetrating brushes (Figure 2) has a power-law-like time dependence $\ln G(t) \sim [\ln(t/t_{Ae})]^\beta$ with $^1/_2 < \beta < 2$. In a real block copolymer lamellar mesophase the junction points are not grafted to the interface (like the ends of a brush) but can, in principle, move along the interface. Below we discuss the transition to this two-dimensional fluidlike behavior at longer time scales.

Different layers in a lamellar state have different moduli. For a perfectly flat layered system the inverse of the total shear modulus $1/G_{tot}$ is the sum of the inverse of the moduli from the A and B interpenetration zones ($1/G_{AI}$ and $1/G_{BI}$) and from the A and B strongly stretched zones, if such exist ($1/G_{AS}$ and $1/G_{BS}$) weighted by the corresponding volume fractions of these zones (ϕ_{AI}, ϕ_{BI}, ϕ_{AS}, and ϕ_{BS})

$$1/G_{tot} = \phi_{AI}/G_{AI} + \phi_{BI}/G_{BI} + \phi_{AS}/G_{AS} + \phi_{BS}/G_{BS} \quad (30)$$

Equation 30 can be understood by analogy with the sequential connection of springs. The lowest modulus controls the sum. This is the reason why in the previous section we have concentrated on the weakest layer—the A interpenetration zone with the highest disentanglement rate (we have assumed that $t_A^* < t_B^*$ as defined by eq 16) $G_{tot} \approx G_{AI}$.

The results of the previous section are valid as long as there is a solidlike layer with finite modulus that acts as

a solid substrate to which the junction points of a copolymer are "grafted". This solidlike substrate is the B layer because we have assumed that the disentanglement process there is slower than in the A layer.

The presence of the solidlike layer is important for the anomalous power-law behavior described in section III. The exponentially rare long-lived entanglements can have a measurable effect only if they link solidlike layers. These long-lived entanglements are also present in melts and concentrated solutions of star polymers, but they do not contribute to elasticity because they are exponentially rare and do not form a connected network. Polymer is able to flow around these "hard bridges".

In the case of a lamellar structure, as soon as solidlike layers "melt", the exponentially long-lived links are no longer effective and the viscoelastic response from the system becomes liquidlike.

The transformation of the solidlike response of a layer at shorter times to liquidlike at longer times, as entanglements are released, is similar to a gel–sol transition. It occurs when the number of unrelaxed entanglements drops to an average of order 1 per copolymer chain. The corresponding relaxation time is (see eq 13)

$$\tau_{relax} \approx \max[t_{Ae} \exp(\nu N_A/N_{Ae}), t_{Be} \exp(\nu N_B/N_{Be})] \quad (31)$$

Above we have assumed that the B block relaxes slower than the A one; therefore, $\tau_{relax} = \tau_B \equiv t_{Be} \exp(\nu N_B/N_{Be})$. This relaxation time τ_{relax} is the time of an elementary step of the two-dimensional copolymer diffusion along the lamellar plane with the diffusion coefficient

$$D_{2d} \approx a_\parallel^2/\tau_{relax} \quad (32)$$

where $a_\parallel$ is the tangential (in plane) tube diameter at the interface.

In the weakly stretched case configurations of polymer chains are nearly isotropic and the degrees of polymerization between entanglements are the same as in the homopolymer melts (for example, $N_e = 180$ for polystyrene). In the strongly stretched case the average distance between entanglements could be significantly different.[26]

B. Triblock Copolymers: Strong Stretching Limit. A very interesting case of a solidlike layer is a lamellar mesophase ($f_i \approx 1/2$) of an ABA triblock copolymer. The middle B layer consists of loops and bridges. In the weakly stretched case pairs of loops with the ends at the opposite interfaces entangle heavily with each other (Figure 5a). In order to release these entanglements, A blocks have to dive into the B domain. This process will control the relaxation of domains (see subsection III.D).

In the strong stretching limit there is a gap in the middle of a B domain with no loops (filled only by bridges).[27-29] Thus in this case there are practically no entanglements between pairs of loops with ends at the opposite interfaces (Figure 5b).

"Melting" of the lamellae for ABA triblock copolymers occurs in the middle B block due to disentanglement of B bridges. On the time scale when B bridges disentangle from each other (to be calculated below) they begin to flow along the lamellae around rare "permanent" loop entanglements. If these "permanent" loop entanglements are rare enough, they do not form a network (they are below their own percolation threshold).

Below we describe the disentanglement modes that require no displacement of A blocks into the B domain (or B blocks into the A domain) but rather the motion of junction points along the interfaces between domains. The time scales considered in this section are longer than the full retraction time of A blocks

$$t > \tau_A \approx t_{Ae} \exp(\nu N_A/N_{Ae}) \quad (33)$$

but still short compared to the time required for A blocks to dive into the B domain [proportional to $\exp(\chi^{1/2} N_A^{2/3})$ as discussed in section III.D]. We discuss two possible disentanglement mechanisms,[30] single-chain motion and collective modes, and demonstrate that the corresponding relaxation times are extremely long.

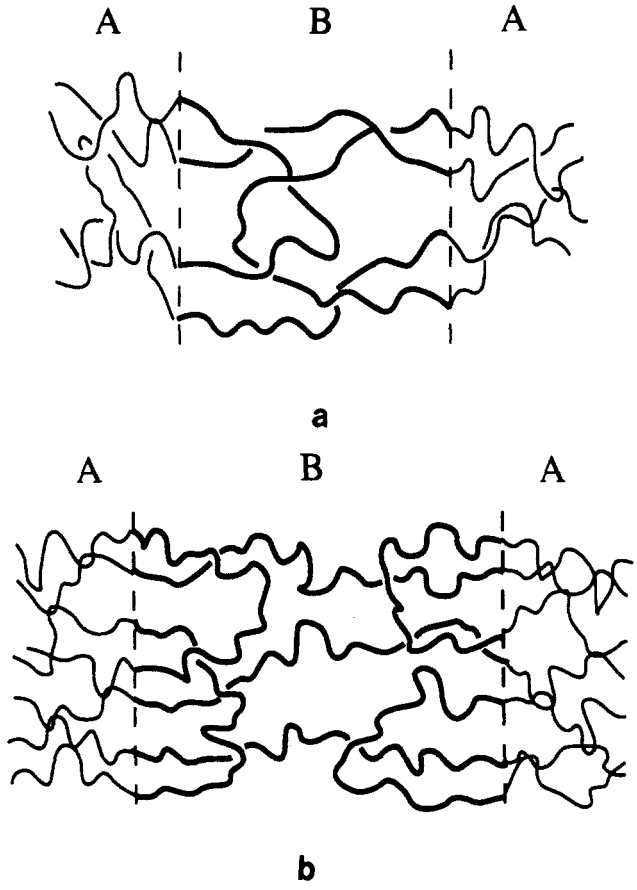

Figure 5. Triblock copolymers in a lamellar mesophase. (a) Entanglements of loops with ends at different interfaces can only be relaxed by moving corresponding A blocks through a B zone (or B blocks through an A zone). (b) In the strong stretching limit for ABA triblock copolymer there is a gap in the middle of a B lamella with no loops (only with bridges).

1. **Single Chain Modes.** Consider the simplest configuration of an entangled pair of bridges CC′ and DD′ in the B region between interfaces I and I′ (Figure 6a). In order for the bridge CC′ to follow the motion of the lower junction point C′ and move to the right, the top junction C has to go around point D in the counterclockwise direction. The projection of the bridge DD′ onto the top interface I is sketched in Figure 6b. The trajectory of the junction point C of bridge CC′ around junction D is indicated by a thin line with an arrow.

A simple configuration of two bridges EE′ and FF′ and a loop GH is shown in Figure 6a. The junction point E of bridge EE′ needs to cover the path shown in Figure 6c in order to follow the lower junction point E′ in its displacement to the right and to disentangle from bridge FF′ and loop GH. Note that junction point E has to go twice around junction G (once on the way to junction point F and once on the way back). It is easy to see that, in the system of high molecular weight triblock copolymers, bridge FF′ and loop GH will be entangled with other loops and bridges. As was shown in our previous publication,[30] the length l of the total path of the junction point E in the

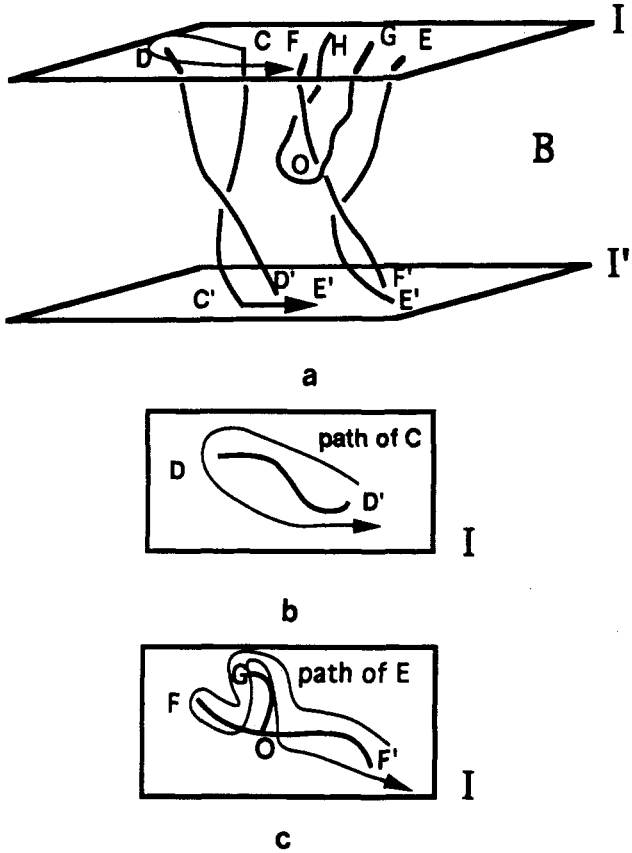

Figure 6. (a) Simple entanglements between middle blocks for a triblock copolymer with junction points localized at the interfaces I and I'. (b) Projection of the middle block DD' (sketched in Figure 6a) onto interface I. Thin line with an arrow indicates the path of junction point C of the bridge CC' around the junction point D. (c) Projection of the bridge FF' and the part GO of the loop GOH (sketched in Figure 6a) onto the interface I. The path of the junction E of bridge EE' required for the disentanglement of this bridge from the bridge FF' and loop GOH becomes significantly more complicated than the path of junction point C in Figure 6b.

top interface I grows exponentially with the number of entanglements per block N_B/N_{Be}

$$l \sim a_{\parallel} \exp(c_2 N_B/N_{Be})$$

where c_2 is a numerical coefficient of order unity. Note that this trajectory is unique and a priori the probability for a junction point E, undergoing a simple diffusion, to find this unique trajectory is exponentially small $\sim\exp(-c_3 l/a_{\parallel})$, where c_3 is another constant of order unity. Therefore, the single-chain disentanglement time is

$$\tau_1 = \tau_A \exp[c_3 \exp(c_2 N_B/N_{Be})] \qquad (34)$$

where τ_A is given in eq 33.

2. Collective Modes. So far we have analyzed the motion of a single bridge assuming others to be fixed. In this subsection we consider collective modes that allow a given chain to disentangle and completely change its configuration with the help of surrounding chains that rearrange appropriately. Below we estimate the fraction of the system that participates in a collective attempt to release an entanglement number s (numbers along the chain start from the nearest interface).

Consider an entanglement between the sections of the chains (bridges or loops) MM' and NN' outlined by the circle in Figure 7. In order to collectively release it, the sections MM' and NN' have to disentangle from their neighbors, while those have to disentangle from their own prospective neighbors, etc. Thus in order to release the

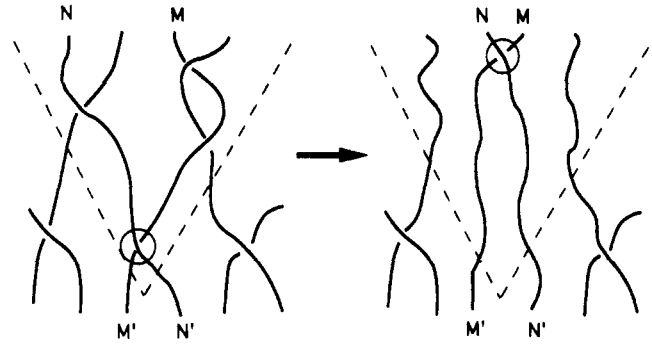

Figure 7. Collective disentanglement mode for the middle blocks of a triblock copolymer.

chosen entanglement (circle in Figure 7), it is necessary to push to the surface all interconnected entanglements inside a cone (dashed line in Figure 7). This cone contains $\sim s^3$ entanglements. As a result of this collective mode, all lines inside this cone are straightened (since all entanglements inside it are pushed to the surface), leading to an increase of free energy (decrease of entropy) of $\sim kT$ per entanglement involved. Therefore, the relaxation time of this collective mode is $\tau_s \sim \tau_A \exp(c_4 s^3)$, where c_4 is a dimensionless constant. The hardest entanglements to be released are located in the middle of the B block with $s = N_B/(2N_{Be})$; therefore, the longest relaxation time of these collective modes is

$$\tau_{col} \sim \tau_A \exp[(c_4/8)(N_B/N_{Be})^3] \qquad (35)$$

For high molecular weight chains both single-chain and collective relaxation times (eqs 34 and 35) are extremely long.

Another mechanism of melting the B layer is by A blocks diving into the B zone (see section III.D for a discussion of this process). All these mechanisms give extremely long relaxation times. This indicates a potential difficulty in achieving an equilibrium configuration of triblock copolymers even significantly above glass transition temperatures of both phases.

V. Defect-Controlled Regime

As we discussed in the previous section, there is a well-defined time scale on which copolymers begin to diffuse along the interface. For unentangled macromolecules this time scale is given by the Rouse time of the slower of the blocks. For entangled diblocks this time scale for the onset of the lower dimensional diffusion along the interface (two-dimensional for the lamellar mesophase and one-dimensional for the cylindrical one) is given by eq 31. For entangled ABA triblocks this time scale is controlled by the shorter of either disentanglement time [single chain (eq 34) or collective (eq 35)] or by the penetration time of an A block through a B lamella (section III.D). Note that, as long as the B block (that for the symmetric mesophase is twice as long as either of the A blocks) does not penetrate an A lamella, the copolymer has to move along the B lamella. The two time scales (penetration of an A block through a B lamella and penetration of a B block through an A lamella) can be separated by many orders of magnitude. Thus the regime we are focusing on in this section is the one with blocks freely diffusing along the interface but unable to move in transverse directions by distances longer than the mesophase period.

For perfectly flat lamellae parallel to the plane of shear, the stress relaxes as soon as the copolymer is able to diffuse along the interface. For example, the relaxation time for diblocks is given by eq 31. As soon as lamellae "melt", they can slide by each other and relax stress.

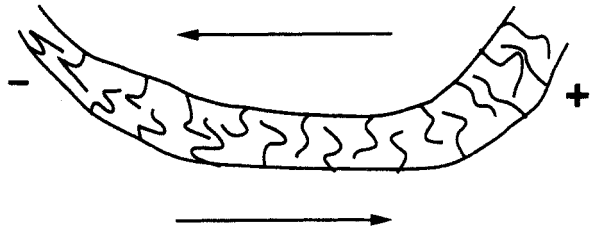

Figure 8. Perturbed distance between interfaces upon a simple shear. In some regions (+) it leads to an increase in the number of blocks per unit interface area. In other regions (−) it leads to a decrease in this interface block density.

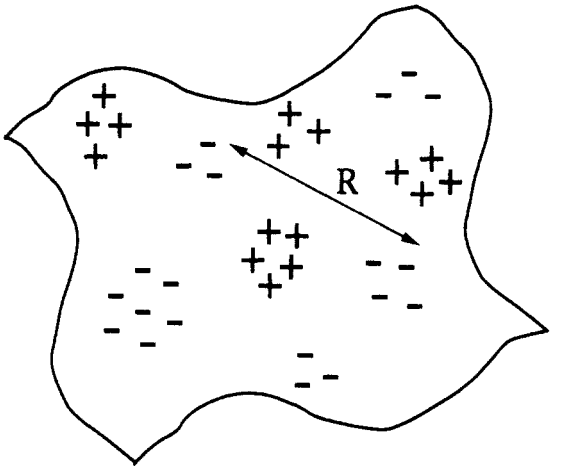

Figure 9. Collective diffusion of copolymer along the interface partially reequilibrates the excess (+) and deficit (−) of the copolymer density per unit interface area.

But in a more general situation, the interface can be oriented by different angles with respect to the shear plane. This can be due to the presence of defects (dislocations, focal conics, etc.). In the case of nonzero angle between the interface and the shear plane, the distance between neighboring interfaces is perturbed by shear (Figure 8). The density of a copolymer melt is fixed, and this change of interface spacing leads to a change in the copolymer density per unit interface. This density is lower in the region of contraction (region "−" in Figure 8) and higher in the region of expansion (region "+" in Figure 8). These distortions lead to stress in the system that can relax only by collective diffusion of copolymer from regions of expansion (+) to regions of contraction (−). Note that bulk density is uniform throughout the system and we are focusing on the surface density per unit interface.

The surface density of blocks can, in principle, be adjusted by changing the interface area without diffusion of copolymers. But in the presence of defects (focal conics, dislocations, etc.) this mode of relaxation of the interface is topologically impossible.

On length scales longer than the separation between defects, the regions of excess and deficit copolymer density per unit interface (regions "+" and "−") are located at random (Figure 9). This is the result of a random orientation of the interface with respect to the shear plane on large length scales.

Let D_c be a collective diffusion coefficient of a copolymer along the interface. During time t the interface density is partially reequilibrated over distances $L(t) \sim (D_c t)^{1/2}$ and therefore over area $A \sim D_c t$ for two-dimensional diffusion [$A \sim (D_c t)^{1/2}$ for one-dimensional diffusion].[31] The unbalanced density and the remaining stress is

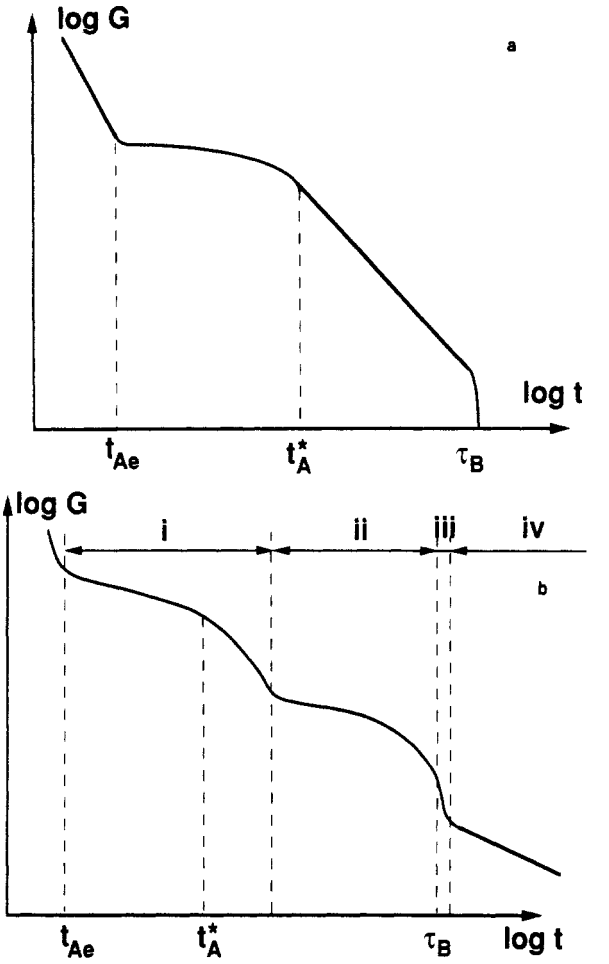

Figure 10. (a) Stress relaxation function for perfectly flat lamellae. (b) Stress relaxation function for a disordered lamellar system.

proportional to $A^{-1/2}$. Thus it is

$$G(t) \sim t^{-1/2} \tag{36}$$

for the lamellar mesophase. Similar considerations for the cylindrical mesophase, where the equilibration can be considered as a one-dimensional process, lead to

$$G(t) \sim t^{-1/4} \tag{36a}$$

Experimentally it is well-established[3-5] that at low frequencies (at long times) the stress relaxation function for a lamellar mesophase satisfies eq 36.

VI. Discussion

A. Perfectly Flat Lamellae. We have analyzed the stress relaxation of block copolymers in a strongly segregated lamellar mesophase. For perfectly flat lamellae of high molecular weight block copolymers we expect to observe the brush-on-brush regime (section III) caused by disentanglement of chains from adjacent lamellae (Figure 10a). This regime should be observed at time scales longer than the glass transition zone for the "faster" lamella A but shorter than the disentanglement time τ_B for "slower" lamella B

$$t_{Ae} < t < \tau_B \tag{37}$$

The early part of this regime ($t_{Ae} < t < t_A^*$) is described by a standard arm retraction mechanism.[7] We have demonstrated that during the latter part of the brush-on-brush regime (on time scales longer than the average disentanglement time of an A block $t > t_A^*$), the fluctu-

ations in the number of entanglements per chain in the interpenetration zone lead to an extremely broad (power-law-like) spectrum of relaxation times and to the stress relaxation function that asymptotically varies as

$$\ln G(t) \sim [\ln(t/t_{Ae})]^{\beta} \quad (38)$$

In the strong stretching limit $\beta = 1/2$, while in the weak stretching limit $\beta = 2$. In a typical experimental situation β must be somewhere between the two limits ($1/2 < \beta < 2$) and, therefore, we expect a power-law-like time dependence of the stress relaxation function ($\beta = 1$ corresponds to a pure power law).

The brush-on-brush regime is cut off by the "melting of a lamella" (section IV) at a disentanglement time τ_B for the slower block (lamella B). For perfectly flat lamellae at longer times ($t > \tau_B$), one should observe a liquidlike response.

B. Disordered Lamellar Systems. In a typical bulk block copolymer sample, lamellae are not perfectly flat. There is always a certain amount of disorder in the lamellar orientation. In addition, there are usually structural defects (dislocations, focal conics, etc.) that make it quite difficult to achieve perfect order even by applying large shear strains.

In a perfectly flat layered system the weakest layer (layer A) always controls the modulus. For systems with disordered lamellar structures, the simple equations for the total modulus (i.e., eq 30) are not applicable any more. As the ratio of the moduli of the A and B phases in a disordered lamellar system becomes very small, the stress is being supported by the stronger layer (B lamellae). The value of the ratio of the two moduli G_A/G_B at which the harder layer (B) becomes important depends on how disordered the layers are. The amount of disorder in the lamellar orientation can be characterized by the ratio of the lamellar thickness h and the typical radius of curvature R for the layer (or the average distance between defects). For systems with flatter layers (smaller ratio h/R), the harder phase (B) becomes important at a lower ratio of the moduli G_A/G_B.

The stress relaxation function for the disordered lamellar system (Figure 10b) can have the following regimes:

(i) Brush-on-brush regime for the faster phase (A). Just as for perfectly flat lamellae, on different time scales, determined by the average disentanglement time t_A^* for A block, the stress relaxations occur either by conventional arm retraction ($t < t_A^*$) or by fluctuation-controlled ($t > t_A^*$) mechanisms. But these regimes are cut off at the modulus level determined by the amount of disorder in the lamellar orientation (by the ratio of the lamellar thickness and the typical radius of curvature for the layer h/R) and by the ratio of the moduli of the two phases G_A/G_B at the time scale of this crossover.

(ii) Brush-on-brush regime for the slower phase (B). The stress relaxation occurs by conventional arm retraction of B blocks ($t < \tau_B$ where τ_B is the relaxation time for lamella B). The modulus can be reduced by some geometric factor $g(h/R)$ depending on the disorder in lamellar orientation (h/R). This regime ends at the disentanglement time for the B block τ_B by the "melting of a lamella" mechanism described in section IV.

(iii) Two-dimensional flow regime. At the end of regime ii copolymer is completely disentangled and can diffuse along the layers. At this time scale layers can begin to flow one over another, but at some length scale R, this flow encounters defects in lamellar structure (Figure 9) and stress relaxation enters regime iv.

(iv) Defect-controlled regime. At long times the stress relaxation is controlled by the defects in lamellar orientation. In section V we addressed one possible mechanism of relaxation in this regime—diffusion-controlled annihilation. It leads to the stress relaxation function decaying as a power of time. For the disordered lamellar mesophase we predict

$$G(t) \sim t^{-1/2}$$

This behavior has been experimentally observed at low frequencies.[3-5] The details of stress relaxation in this regime will be discussed in a future publication.[6]

The sequences of regimes for the disordered lamellar system, described above and sketched in Figure 10, is only one possible scenario for a relatively low amount of disorder (low h/R).

If the system is more disordered, the crossover to the modulus controlled by the slow phase (B) would occur at earlier times. It can be either in the earlier part of regime i or even in the glassy region of stress relaxation function. We do not list other possible sequences of regimes due to space limitations.

C. Effects of Polydispersity. Another important issue we would like to discuss is the effect of polydispersity. Block copolymers are usually prepared by anionic polymerization that is characterized by a Poisson distribution of molecular weights of the resulting polymers.[32] This distribution gives a dispersion in the degree of polymerization of order $N^{1/2}$ and leads to a dispersion in the number of entanglements of order $N^{1/2}/N_e$. This dispersion is narrower than that due to thermal fluctuations $(N/N_e)^{1/2}$, but there are several effects enhancing the role of polydispersity in the block copolymer systems:

(i) In the case of strong stretching the longer chains are pushed out into the interpenetration zone.[33]

(ii) In some cases the high molecular weight tail of the distribution obtained in anionic polymerization can significantly deviate from the Poisson.

Acknowledgment. The authors thank F. Brochard-Wyart, R. H. Colby, A. N. Semenov, and T. A. Witten for helpful discussions and L. Leibler for constructive criticism.

References and Notes

(1) *Block Copolymers: Science and Technology*; Meier, D. J., Ed.; MMI Press/Harwood Academic Publishers: New York, 1983. *Developments in Block Copolymers*; Goodman, I., Ed.; Applied Science: New York, 1982; Vol. 1; 1985; Vol. 2.
(2) Bates, F. S.; Fredrickson, G. H. *Annu. Rev. Phys. Chem.* **1990**, *41*, 525 and references therein.
(3) Rosedale, J. H.; Bates, F. S. *Macromolecules* **1990**, *23*, 2329.
(4) Bates, F. S.; Rosedale, J. H.; Fredrickson, G. H. *J. Chem. Phys.* **1990**, *92*, 6255.
(5) Koppi, K. A.; Tirrell, M.; Bates, F. S.; Almdal, K.; Colby, R. H. *J. Phys. II. (Fr.)* **1992**, *2*, 1941.
(6) Obukhov, S. P.; Rubinstein, M., to be published.
(7) Witten, T. A.; Leibler, L.; Pincus, P. *Macromolecules* **1990**, *23*, 824.
(8) Meier, D. J. *J. Polym. Sci.* **1969**, *C26*, 81.
(9) Leary, D. F.; Williams, M. C. *J. Polym. Sci.* **1970**, *B8*, 335.
(10) Helfand, E. *Macromolecules* **1975**, *8*, 552.
(11) Helfand, E.; Wasserman, Z. R. *Macromolecules* **1976**, *9*, 879.
(12) Helfand, E.; Tagami, Y. *J. Chem. Phys.* **1971**, *56*, 3592; *J. Polym. Sci.* **1971**, *B9*, 741.
(13) Semenov, A. N. *Zh. Exp. Theor. Phys.* **1985**, *88*, 1242; translated in *Sov. Phys. JETP* **1985**, *61*, 733.
(14) Milner, S. T.; Witten, T. A.; Cates, M. E. *Europhys. Lett.* **1988**, *5*, 413; *Macromolecules* **1988**, *21*, 2610.
(15) Doi, M.; Edwards, S. F. *The Theory of Polymer Dynamics*; Oxford University Press: Oxford, U.K., 1986.
(16) de Gennes, P.-G. *J. Phys. (Fr.)* **1975**, *36*, 1199.
(17) Pearson, D. S.; Helfand, E. *Macromolecules* **1984**, *17*, 888.
(18) Ball, R. C.; McLeish, T. C. B. *Macromolecules* **1989**, *22*, 1911.

(19) Doi, M.; Kuzuu, N. Y. *J. Polym. Sci., Polym. Lett. Ed.* **1980**, *18*, 775.
(20) Curro, J. G.; Pincus, P. *Macromolecules* **1983**, *16*, 559. Curro, J. G.; Pearson, D. S.; Helfand, E. *Macromolecules* **1985**, *18*, 1157.
(21) Doi, M. *J. Polym. Sci., Polym. Lett. Ed.* **1981**, *19*, 265; *J. Polym. Sci., Polym. Phys. Ed.* **1983**, *21*, 667.
(22) Rubinstein, M. *Phys. Rev. Lett.* **1987**, *59*, 1946.
(23) Marrucci, G. *J. Polym. Sci., Polym. Phys. Ed.* **1985**, *23*, 159.
(24) Leibler, L.; Rubinstein, M.; Colby, R. H., to be published.
(25) Helfand, E. *Macromolecules* **1992**, *25*, 492.
(26) Boris, D.; Rubinstein, M., to be published.
(27) Ligoure, C.; Leibler, L.; Rubinstein, M., submitted to *Macromolecules*.
(28) Halperin, A.; Zhulina, E. B. *Prog. Colloid Polym. Sci.* **1992**, *90*, 156.
(29) Joanny, J. F.; Johner, A. *J. Chem. Phys.* **1992**, *96*, 6257.
(30) Obukhov, S. P.; Rubinstein, M. *Phys. Rev. Lett.* **1990**, *65*, 1279.
(31) This equilibration process is called diffusion-controlled annihilation. It was studied by the following: Burlatskii, S. F. *Theor. Exper. Chem. (in Russian)* **1978**, *14*, 483. Zeldovich, Ya. B.; Ovchinnikov, A. A. *Chem. Phys.* **1978**, *28*, 215. Kang, K.; Redner, S. *Phys. Rev. Lett.* **1984**, *52*, 955. For diffusion on a manifold with fractal dimension d_f, the density of remaining objects decays as $t^{-d_f/4}$.
(32) Flory, P. J. *Principles of Polymer Chemistry*; Cornell University Press: Ithaca, NY, 1953.
(33) Milner, S. T.; Witten, T. A.; Cates, M. E. *Macromolecules* **1989**, *22*, 853.